analytical chemistry

pubs.acs.org/ac Article

High-Sensitivity and Trace-Amount Specimen Electrochemical Sensors for Exploring the Levels of β-Amyloid in Human Blood and Tears

Yu-Rong Wang, Han-Chien Chuang, Adarsh Tripathi, Yu-Lin Wang, Mei-Lan Ko, Ching-Cheng Chuang, and Jung-Chih Chen*

Cite This: *Anal. Chem.* 2021, 93, 8099−8106 Read Online

ACCESS | Metrics & More | Article Recommendations

ABSTRACT: As the occurrence of Alzheimer's disease (AD) has increased, the detection and treatment of AD have become global social issues. Effective early detection and wide-range screening of AD allow patients to gain early control and delay brain degeneration. For these reasons, we choose electrochemical sensors to complete the detection task. Although bio-electrochemical technology for antibody and antigen sensing is not a new technology, considering the scarcity of tear samples for dementia and since the existing AD detection techniques are highly invasive and expensive for subjects, we have to use the traditional detection techniques for the early screening of Alzheimer's disease via trace-amount specimens. An AD-related protein in the eye is thought to be an important biomarker for early detection. To carry out detection using tear samples as a test specimens, a tear collection device was developed in this study that extracted 10 μL of tear fluid from a tear Schirmer strip. In this research, we distinguished healthy people in different age groups and detect Aβ in both tear and blood samples. We developed a biosensor, which could detect Aβ in tear specimen from 1 to 100 pg/mL. Also, this biosensor is inexpensive, disposable, and easy to use. In our result, the concentration of Aβ in tears was approximately 10 times more than that in blood. This study demonstrates the feasibility and prospects of future screening for AD-associated biomarkers by a dynamic comparison between blood and tears.

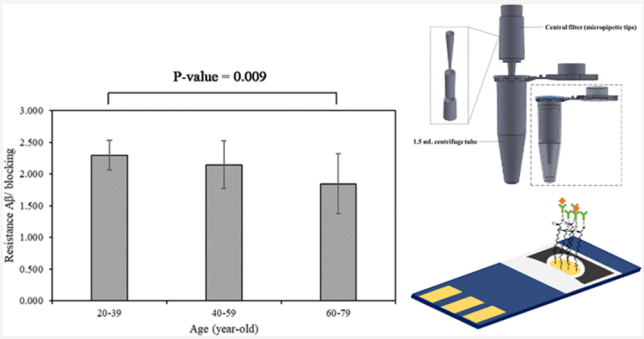

According to the 2015 Global Dementia Report, on an average, one person every 3 s is diagnosed with dementia. The report also estimated that the total population suffering from dementia will increase to 113.5 million people in 2050.[1] Among all of the reported cases worldwide, Alzheimer's disease (AD) is the most common type of dementia, accounting for 60−70% of all dementia cases.[2] Currently, among many kinds of hypotheses, the "amyloid-like hypothesis" is the most accepted pathogenic mechanism for AD progression. This hypothesis focuses on two major related pathological proteins. One is the amyloid precursor protein (APP) and the other is the Tau protein.[3]

APP is a transmembrane protein that is abundantly distributed on brain nerve cells. β-Secretase is first cleaved at the carboxyl terminus of the amyloid precursor protein to form the carboxyl-terminal fragment of the amyloid precursor protein. Subsequent further cleavage by γ-secretase yields a peptide fragment of 39−43 amino acids in length. These peptide fragments are referred to as β-amyloid peptides. The most abundant β-amyloid (Aβ) peptides in the body are $A\beta_{1-40}$ and $A\beta_{1-42}$. $A\beta_{1-42}$ is more likely to be decomposed as compared to $A\beta_{1-40}$, which can rapidly aggregate into an oligomeric peptide in the brain.[4] A fibrillary Aβ stack, followed by final plaques, is formed in the brain, which causes neuronal death. Therefore, $A\beta_{1-42}$ is the most important peptide in the pathway leading to AD. In addition, the toxicity produced during the process of aggregation of Aβ to form plaques triggers excessive phosphorylation of the Tau protein. Once the Tau protein is hyperphosphorylated, it begins to detach from the microtubules and accumulates in the synapse. This disrupts the neuron signaling pathway and ultimately leads to the death of neurons.[5,6] Currently, the US Food and Drug Administration approves the usage of cholinesterase inhibitors and NMDA receptor antagonists for the treatment of AD.[7,8]

Received: November 27, 2020
Accepted: May 17, 2021
Published: May 28, 2021

https://doi.org/10.1021/acs.analchem.0c04980
Anal. Chem. 2021, 93, 8099−8106

However, currently available drugs for the treatment of AD can only decelerate the occurrence of symptoms and delay the progression of the disease but are unable to completely cure AD.

Neuroimaging techniques allow for the immediate observation of changes in the structure and function of the brain and have the advantage of being noninvasive and accurate. The extent of Aβ accumulation and the metabolism of brain cells are monitored using Pittsburgh Compound-B positron emission tomography (PIB-PET) and fluorodeoxyglucose positron emission tomography (FDG-PET). Magnetic resonance imaging (MRI) and computed tomography (CT) scans are used to observe the shrinkage of the cortical region of the brain. Nevertheless, the major disadvantages of neuroimaging are that it is expensive and is prone to radiation exposure. Therefore, neuroimaging techniques are not suitable for early detection of AD.

Analysis of concentrations of Aβ and Tau proteins is one of the ways to diagnose AD. In 2018, NIA-AA included Aβ and Tau protein analysis from cerebrospinal fluid (CSF) as one of the diagnostic parameters for AD.[9] After obtaining CSF by lumbar puncture, the total amount of Tau protein, phosphorylated Tau protein, and Aβ peptide in CSF were detected by enzyme-linked immunosorbent assay (ELISA). Although there are many types of Aβ peptides, $A\beta_{1-40}$ and $A\beta_{1-42}$ are better indicative of AD because $A\beta_{1-42}$ in CSF is directly related to Aβ in the brain.[10−13] A decrease in the concentration of $A\beta_{1-42}$ in CSF may be related to the accumulation of Aβ in the brain.[14] Previous studies have shown that although the concentration of $A\beta_{1-40}$ in CSF of patients with AD is not much different from that of the healthy control group, a significant decrease can be found by comparing the ratio of $A\beta_{1-42}$ to $A\beta_{1-40}$. The ratio of $A\beta_{1-42}$ to $A\beta_{1-40}$ is more reliable as compared to $A\beta_{1-42}$ alone because the ratio can compensate for differences in peptide levels between individuals.[15,16] Clinical studies have confirmed that the ratio of $A\beta_{1-40}$ to $A\beta_{1-42}$ in the brain of normal people is 9:1. Since AD is caused due to the accumulation of $A\beta_{1-42}$, the ratio of $A\beta_{1-40}$ to $A\beta_{1-42}$ approaches 1:1 in AD patients.[17−19] The biochemical examination of cerebrospinal fluid can directly reflect the biochemical changes in the brain. However, as mentioned before, this is an invasive test and the cost of performing ELISA is high.

Since the optic nerve is one of the 12 pairs of cranial nerves, changes in the eye can potentially reflect changes in the brain. Many researchers have been investigating ophthalmic biomarkers in relation to AD, including visual changes, eye movements, pupillary responses, ocular images, and biochemical and microRNA changes in ophthalmic fluids.[20−22] These biomarkers are expected to help develop the early detection strategies for AD. However, ophthalmic detection is mostly based on optics at present. Previous studies have indicated deposition of Aβ on the lens and the retina.[23−27] One of the recent studies in 2019 explored the aspect of extraction of vitreous humor from the eye for quantification of Aβ and Tau proteins. An intelligence state check scale for cognitive assessment was performed simultaneously. The results showed that people with poor cognitive functions had significantly reduced amounts of Aβ and Tau proteins. This gave further evidence that the ocular proteins are important for the early detection of AD.[28]

A biosensor based on electrochemical impedance spectroscopy is a device that converts the changes in physical or chemical diversity into an electrical signal. Substances such as antigens, proteins, microorganisms, glucose, chemicals, and drugs can alter the electrode surface and affect the signal.[29−33] Currently, the application of electrochemical sensors is more advanced in clinical testing. Electrochemical sensors have high sensitivity and rapid response rates. Moreover, electrochemical sensors require less specimen volume as compared to other chemical detection methods, such as HPLC, fluorescence immunoassay, immunomagnetic reduction assay, etc. Although a ospecimen of tears and blood can be diluted to meet the demand for the amount of detection assay, the concentration of target protein in the specimen might not reach the detection limit. Therefore, detection of $A\beta_{1-42}$ and Aβ oligomers using an electrochemical sensor has been performed recently.[34−37] Since the currently available AD detection methods have individual flaws, using electrochemical technology to examine minimally invasive samples, such as blood and tears, is a way to reduce the detection cost and widen the detection limits for testing in the future. Tears contain many physiological and chemical components similar to human blood, such as cholesterol, sodium, potassium, and blood sugar. To accomplish the aims of early detection and wide-range screening of AD-associated biomarkers, our study reveals the results from healthy people of different age groups and a novel biosensor for quantitative detection. We use a disposable screen-printed-electrode that contains three kinds of different material electrodes. This screen-printed-electrode is different from that used in the traditional three-electrode electrochemical method. In the traditional method, there is a need to prepare an environment to contain three kinds of electrodes, but this screen-printed-electrode contains all electrodes on the same flat. Also, the specimen volume requirement is less than that of the traditional examination method. However, to facilitate the acquisition of specimens, the construction of a simple device for extracting tear samples from Schirmer strips is important. Furthermore, this study also monitors the progression of Aβ alteration in tear and blood to help better understand this age-associated disease.

MATERIALS AND METHODS

Chemicals and Materials. 11-Mercaptoundecanoic acid (MUA), potassium hexacyanoferrate [$K_3Fe(CN)_6$], potassium hexacyanoferrate [$K_4Fe(CN)_6$], potassium chloride (KCl), *N*-hydroxysuccinimide (NHS), and 2-(*N*-morpholino)-ethanesulfonic acid (MES) were purchased from Sigma-Aldrich. 1-Ethyl-3-(3-dimethylaminopropyl)carbodiimide hydrochloride (EDC) and ethanolamine were purchased from Alfa Aesar and JT Baker, respectively. A mouse monoclonal antibody MOAB-2, which can detect multiple $A\beta_{1-40}$ and $A\beta_{1-42}$ conformations including unaggregated and oligomeric and fibrillar forms, was purchased from Merck. All other chemicals were analytical grade and used without further purification. Phosphate-buffered saline (PBS, 1×, pH 7.2) was purchased from Fisher Scientific. Ultrapure water (18 MΩ cm) was produced from a Milli-Q water purification system and was used throughout the experiments.

Electrochemical Measurements. The disposable screen-printed-electrodes (SPEs) were purchased from Vida Bio Technology Co. Ltd. The SPEs consisted of a three-electrode system containing a 1.68 mm^2 Ag/AgCl electrode, a 5.2 mm^2 Au electrode, and a 54 mm^2 carbon electrode, and the total area of electrodes is 40 mm × 12.5 mm. These three-electrode systems were chosen as reference, working, and counter

https://doi.org/10.1021/acs.analchem.0c04980
Anal. Chem. 2021, 93, 8099−8106

electrodes, respectively. Moreover, the working electrode was composed of a highly sensitive nanostructure based on 3D deposited gold nanoparticles. All electrochemical measurements were performed using a CHI920D electrochemical instrument (CH Instruments, Inc.) connected to a computer for data collection.

Data Analysis and Statistical Method. The data was calculated by fitting the equivalent circuit with the built-in tool of Zsim in CHI920D. We used the coefficient of determination and standard deviation to deliberate the accuracy of our standard calibration curve. Blood and tear samples were analyzed by standard deviation and Student'S *t*-test. *P*-value were utilized for statistical significance.

Preparation of the Tear Sample Collection Device. Currently, the commonly used methods to obtain human tear fluids include the use of Schirmer strips and capillary tubes. In this study, the Schirmer strip method was chosen to collect human tear fluid samples over the capillary tube method as the capillary tube method requires a skilled professional to operate. For this reason, a new device was also designed to collect human tear fluid samples. This device consisted of an external 1.5 mL centrifuge tube and an internal central filter. The central filter is an important component of this device because it is used to separate the tear fluid sample on the Schirmer strip. To fabricate the central filter, 1000 μL micropipette tips were first cut into three parts and then restructured in a unique manner. After reconstitution, the resultant length of the central filter was 3 cm. Figure 1 shows the detailed structure of this tear fluid sample collection device.

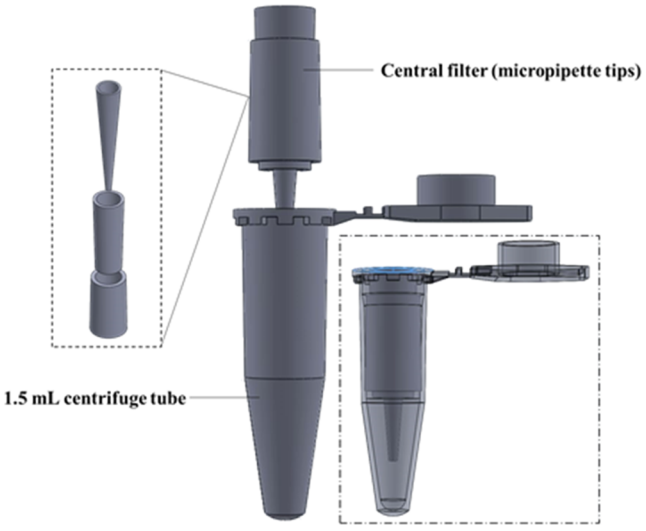

Figure 1. Tear fluid sample collection device.

Tear and Blood Sample Collection. To determine the concentration of Aβ in healthy subjects of different ages, this study included 50 healthy volunteers from the age of 20 to 79 years without any chronic diseases like dry eye, diabetes, peripheral vascular disease, and Alzheimer's disease. The number of male and female subjects was 13 and 37, respectively. Figure 2 shows the number and gender distribution in different age groups. Both tear fluid and blood samples were collected from every volunteer within a 3 h time period. First, the tear fluid samples were collected by inserting the Schirmer strip into the lower conjunctival sac without anesthesia. While collecting tears, the volunteers

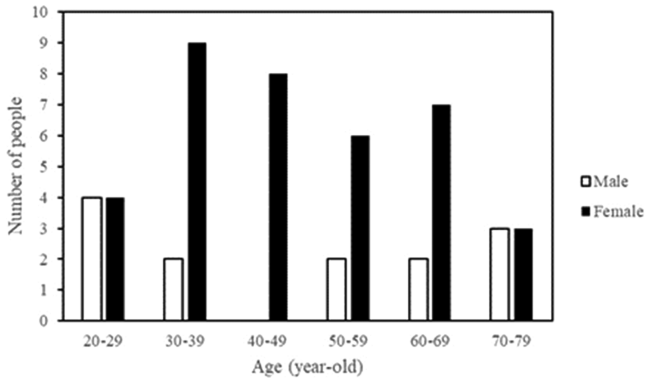

Figure 2. Distribution of healthy volunteers from different age groups.

closed their eyes until the Schirmer strip absorbed tear fluid till the 20 mm mark, and then, the strips were removed immediately. After the strips were removed from the eyes, they were rolled up forcefully and put into the tear fluid collection device. The samples were then centrifuged at 13 000 rpm for 5 min. After centrifugation, the central filter device was removed. The tear fluid samples get separated from the strips and are collected at the bottom of the sterile 1.5 mL centrifuge tube. The samples were stored at −20 °C before use. Next, 3 mL blood samples were collected from the arms of the volunteers in tubes containing sodium heparin to avoid coagulation. The details of the participants and test samples in the study were collected by the Institutional Review Board of National Taiwan University Hospital Hsin-Chu Branch (NTUHHCB-IRB) (NTUHHCB 106-075-E).

Standard Aβ Solution Preparation. To prepare the standard Aβ solution, lyophilized peptide powders of Aβ_{1-40} and Aβ_{1-42} were directly dissolved in 80 μL of NH_4OH (1%), diluted to a final concentration of 1 mg/mL using 1× phosphate-buffered saline, and then immediately stored at −20 °C. Before the experiment, the Aβ_{1-40} and Aβ_{1-42} stock solutions were diluted to various working concentrations, including 10 μg/mL, 1 μg/mL, 100 ng/mL, 10 ng/mL, 1 ng/mL, 100 pg/mL, 10 pg/mL, and 1 pg/mL. The Aβ_{1-40} and Aβ_{1-42} stock solutions contain both monomeric form and oligomeric form.

Fabrication of the Electrochemical Immunosensor. The schematic diagram of the surface modification procedure for the immunosensor is illustrated in Figure 3. To ensure the cleanliness of the working electrode surface, the surface was rinsed with DI water before using the electrode. Then, 10 μL of 10 mM 11-MUA solution (prepared in 99.5% ethanol) was dropped onto the gold working electrode to form self-assembled monolayers (SAMs) on the gold electrode. The modified electrode was rinsed with absolute ethanol to remove unbound and unwanted particles. To activate the carboxyl group (R-COOH) for antibody coupling, a solution containing 30 μL of EDC (10 mM) and NHS (10 mM) in 25 mM MES (pH 5.5) was added onto the modified electrode for 1 h and then rinsed with DI water. The immobilized SAM with activated carboxyl groups was further inoculated with 30 μL of a monoclonal antibody solution (10 μg/mL) and incubated for 1 h and then rinsed with 1× PBS solution. Finally, 50 μL of an ethanolamine solution (0.1 M) was utilized to inactivate the NHS ester so that it would not react with antibodies, therefore minimizing the influence of nonspecific binding. Finally, 10 μL of various concentrations of Aβ_{1-40} peptide solution or tear/

https://doi.org/10.1021/acs.analchem.0c04980
Anal. Chem. 2021, 93, 8099−8106

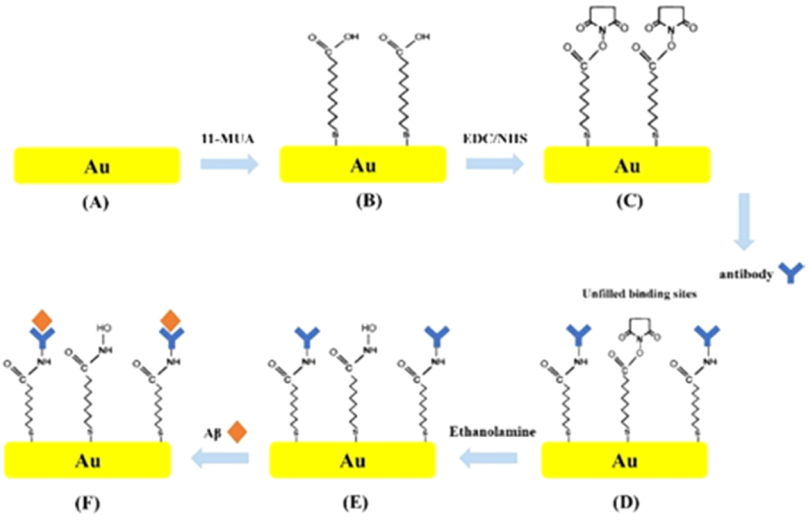

Figure 3. Schematic diagram of the electrode surface modification process.

blood sample was dropped onto the sensor and incubated for 2 h to ensure specific binding between the antibody and the antigen.

Electrochemical Measurements. The electrochemical measurements utilized in this work include cyclic voltammetry (CV) and electrochemical impedance spectroscopy (EIS) analysis. Both electrochemical measurements were carried out in the presence of a 5 mM ferri/ferrocyanide redox couple ($[Fe(CN)_6]^{3-/4-}$) in a 0.1 M KCl buffer solution. For cyclic voltammetry measurements, the electrical potential was scanned from −0.2 to +0.6 V, with a scan rate of 100 mV/s. For electrochemical impedance spectroscopy, a small amplitude AC signal was applied to the working electrode, resulting in a response frequency. The analysis of AC voltage and current response showed the impedance behavior of the working electrode. In our experiment, 0.15 V DC power and 5 mV AC power were applied for impedance measurement of frequencies ranging from 0.02 Hz to 100 kHz.

RESULTS AND DISCUSSION

Electrochemical Characterization of Different Modification Steps. Electrochemical characterization of the stepwise modified electrode fabrication process was carried out by CV and EIS using a 5 mM redox couple reagent. Figure 4I shows the cyclic voltammograms of different modification steps. A couple of redox peaks were found at the bare gold electrode, and the mean of bare gold redox peaks (peak (A)) was the working potential for our EIS measurements. The current peak clearly decreased at each modification step, and at the antibody modification step, no redox peaks were observed. To pass a current between the electrodes and the reagent, electrons were transported through the working electrode surface, reagent, and the counter electrode. Due to electron transfer efficiency, modification of the working electrode created a barrier for electron transport, which affected the magnitude of the peak redox current. The results of EIS measurements were analyzed by the Randles model for equivalent circuit analysis, which is shown in Figure 4II. The Randles model consists of resistors, capacitors, and Warburg components, where R_{ct} is the electron transfer impedance caused because of the attachment on the modified electrode. This is the main component that we used to calculate our tear and blood sample results. R_s is the resistance caused by

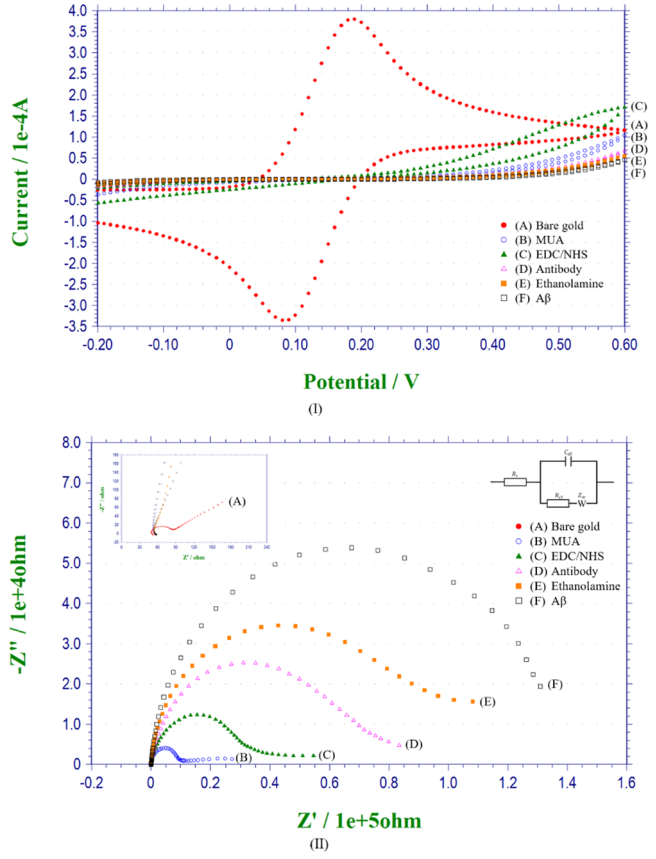

Figure 4. (I) CV of the gold electrode on SPEs at different modification steps. (II) Nyquist plot of each modified layer. The electrode was recorded in a 5 mM redox probe $[Fe(CN)_6]^{3-/4-}$ in 0.1 M KCl. The inset circuit (Randles model) represents our equivalent circuit. R_s is the solution resistance, C_{dl} is the double-layer capacitance, R_{ct} is the charge transfer resistance, and Z_w is the Warburg impedance.

dynamic solution, which we used to investigate electron transfer impedance of a ferri/ferrocyanide redox couple reagent. C_{dl} represents the double layer capacitance between the gold electrode and our redox reagent, and Z_w represents the Warburg element that describes mass transport at different frequencies. The unmodified electrode surface was very clean

https://doi.org/10.1021/acs.analchem.0c04980
Anal. Chem. 2021, 93, 8099−8106

and was tested to have great conductivity. The semicircle on the impedance map was small, which shows that the electrons were easily transferred this time, resulting in very low impedance. Figure 4II demonstrates EIS measurement characteristics for each modification step. Curve (A) represents the impedance of the working gold electrode during the formation of the first layer of SAM from 11-MUA. MUA has a high negative charge, and the presence of SAM prevents the easy transfer of electrons to the electrode surface. Thus, its impedance is much larger than that of the bare electrode. Curve (B) represents impedance after EDC/NHS modification. EDC was used to activate the thiol group of 11-MUA and, in conjunction with NHS, could protect the carboxyl group of the antibody. An increase in impedance at this step indicates that the carboxyl group has been activated to form an NHS ester group. Curve (C) represents impedance after the Aβ antibody was immobilized on the electrode. After the antibody was immobilized, the electrode surface structure began to thicken. Thus, electrons were not easily transferred to the electrode surface. Curve (D) represents impedance after blocking with ethanolamine. This step served to deactivate the NHS ester that was not attached to the antibody. Unspecific binding of the target antigen was also prevented by this step. Curve (E) demonstrates that the increase in impedance after blocking was caused due to the conjugative specificity of Aβ and the antibody.

Tear Fluid Collection. In most clinical tear tests, the general method for collecting tears is to use capillary tubes. The advantage of capillary collection is that we can obtain tear samples directly without the need for dilution or centrifugation. However, this method is more difficult for collecting tears, not only because collecting tears by capillary requires a trained professional but also because of the human fear of the capillary touching the eyes. In this study, tears were collected by Schirmer strips and centrifuged in a tear collection device to avoid the tears getting absorbed back into the strips. The average weight of the tears absorbed on a 20 mm strip was about 13 mg. After centrifugation at 13 000 rpm, a 1.5 mL centrifuge tube contained approximately 10 mg of tear sample at the bottom. The density of tear fluid is 1.005 g, which means that approximately 10 μL of the tear sample can be obtained from each Schirmer strip after centrifugation.

Analysis of a β-Amyloid Standard Solution. Our gold-based electrode immunosensor was designed to measure different amyloid concentrations. The resistance responses due to Aβ were recorded at frequencies ranging from 0.02 Hz to 100 kHz. Before the measurement of volunteer samples, confirming the efficacy of the modified electrode was necessary. We tested not only the positive control but also the negative control. We tested PBS with the fully modified electrode, and the resistance ratio was 1.015, which meant that the resistance is nearly unchanged when testing only PBS. To make blood and tear measurement data more relevant, an Aβ standard calibration curve was also necessary. Figure 5 shows the calibration curve obtained due to the correlation of Aβ_{1-40} concentration and resistance response. These calibration curves show the detection limit of the biosensor. The concentration of Aβ was in the range of 1 pg/mL to 1 ng/mL, indicated by the red line in Figure 5. Although this correlation was a nonlinear relationship, we could still produce a conversion formula for the range of 1 pg/mL to 1 ng/mL with a correlation coefficient of 0.9959. Moreover, the Aβ biosensor fabricated in this study still had a linear relationship

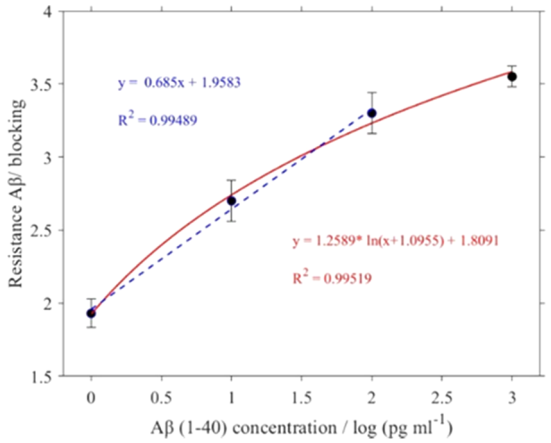

Figure 5. Correlation between Aβ concentrations and resistance changes. Calibration curves for Aβ_{1-40} over the concentration ranges of 1−100 pg/mL (blue line) and 1 pg/mL to 1 ng/mL (red line). The error bars represent the standard deviation of the tests with the same concentration.

in the range of 1−100 pg/mL, which meant that the difference in impedance growth was fixed for every decade of increase in the representative concentration with a correlation coefficient of 0.99489, as shown by the blue line in Figure 5. However, Figure 5 also indicates that the measurement at 1 ng/mL had deviated from the linear relationship of the blue line. Therefore, we could assume that the biosensor approached saturation after 100 pg/mL. In short, the result obtained from the proposed fabrication process of our electrodes covered a wide range of Aβ concentrations and indicated relatively high sensitivity and a low detection limit. Moreover, the Aβ standard solution used in our research contains both monomeric form and oligomeric form, as the Aβ in biological samples. In addition, the linear range included the applicable region and the peptide forms for detecting target samples, which means that the sample can be used without being condensed or diluted.

Human Tear and Blood Analysis. As mentioned before, Aβ is an important peptide related to Alzheimer's disease, and noninvasive sample analysis is important for current research. To evaluate suitable sensors for practical applications, our sensor was applied for the detection of Aβ in human-derived specimens, which included tear and blood samples from a healthy population. The tear samples used here were collected by centrifuging our tear fluid collection device, as mentioned previously. Blood specimens were tested using the entire blood sample. Figures 6 and 7 show the impedance value distributions of Aβ in tears and blood and are grouped based on age to establish a relationship between age and Aβ content in healthy human specimens. For both tear and blood results, the change in impedance value was calculated by subtracting the R_{ct} value (blocking) from R_{ct} (sample). Antibodies we used in the experiments were analyzed for their specificity in previous studies, and results showed that the antibodies were specific for Aβ_{1-40} and Aβ_{1-42}. As previously mentioned, R_{ct} gradually increased at every step where fabrication materials were added. Therefore, the ΔR_{ct} value of the specimen increased from approximately 20 to 100 kΩ, which indicated that blood and tears contain Aβ peptides that could specifically bind to the Aβ antibody.

Due to physiological differences among humans, chemical or environment factors during the electrode surface modification

https://doi.org/10.1021/acs.analchem.0c04980
Anal. Chem. 2021, 93, 8099−8106

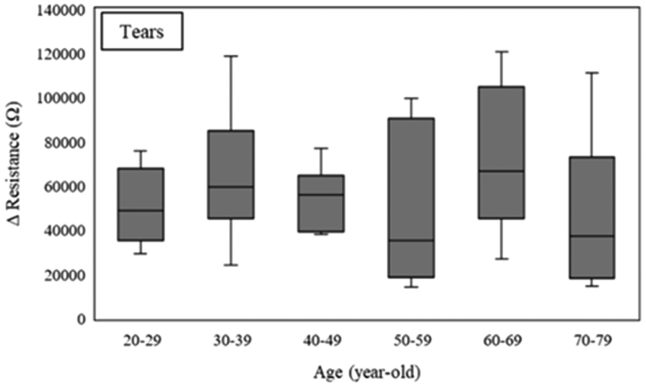

Figure 6. Distribution of β-amyloid peptide impedance values in tear samples from subjects of all ages.

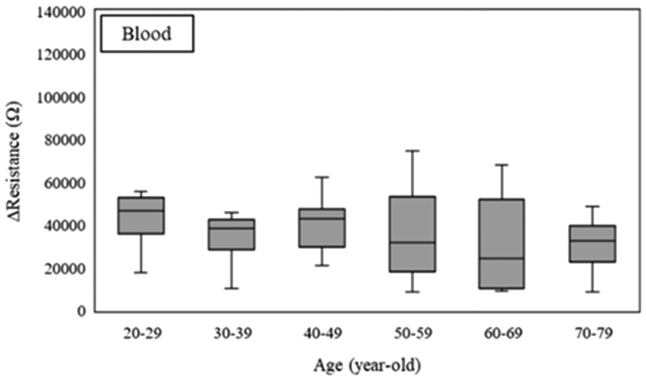

Figure 7. Distribution of β-amyloid peptide impedance values in blood samples from subjects of all ages.

process, and the differences in the subsequent peptide linkages affected by previous modification stages, it is necessary to normalize the measured values of detected resistance. The way to normalize the results is to divide the R_{ct} (sample) value by the R_{ct} (blocking) value. This normalization assumes that the antibody has a fixed probability for specific binding to the target peptide. It is safe to say that the greater the impedance before sample detection, the more the target peptides that subsequently attach to the electrode.

After normalizing the data that was measured by EIS, the growing ratio of impedance value represented the concentration of Aβ in blood and tear samples. The results shown in Figure 8 indicate that Aβ peptide concentration detected in the tear samples was greater than Aβ concentrations in blood samples across all age groups.

Figure 8 shows that the resistance ratios in human tear samples from Aβ measurement results were distributed between 2.4 and 3.2, with an average value of 2.712. In human blood samples, the values were found between 1.9 and 2.3, with an average value of 2.083. The Aβ concentration level of an individual sample can be derived from the linear function as mentioned in the Analysis of a β-Amyloid Standard Solution section. This concentration can be estimated using the following linear equation

$$x = (\mathrm{EIS}(\Omega) - 1.9583)/0.685$$

Using the mean of the EIS analysis results and the above equation, the concentration of Aβ was estimated to be approximately 10 pg/mL in tear samples and approximately 1 pg/mL in blood samples. This result indicates that tears

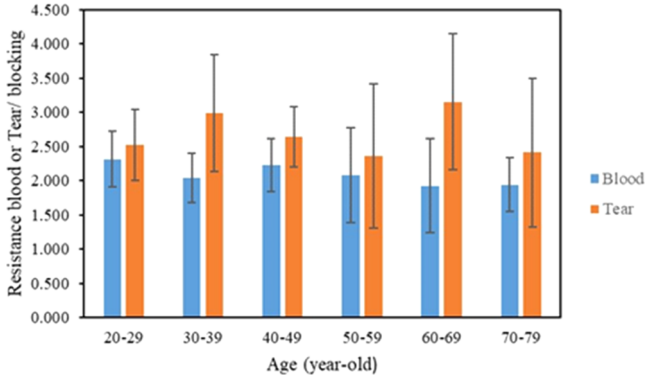

Figure 8. Mean resistance ratios of the tear and blood samples. The ages in each group were separated by 10 years. The error bars represent the standard deviation of the resistance ratio.

contain 10 times the amount of Aβ peptide in blood. Gijs et al. reported that their result in the case of healthy controls also showed Aβ in tears,[38] due to the different tear collection methods and the subjects' average age. We did not test the same concentration.

Although Figure 7 shows the amount of Aβ in blood and tears, we still cannot clearly understand the interdependency of the amount of Aβ and age. However, it is noteworthy that age and resistance ratio distributions shown in Figure 9 indicate

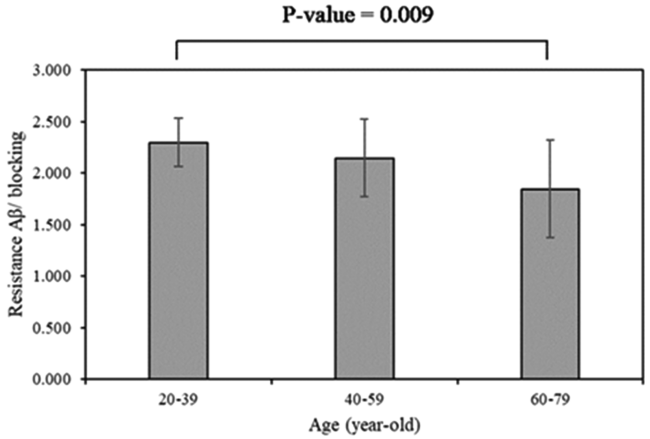

Figure 9. Histogram of the Aβ resistance ratios of the blood sample with reference to age. The age groups were separated by 20 years. The error bars represent the standard deviation of the resistance ratio.

that Aβ content in healthy subjects was inversely proportional to age. Furthermore, the youngest age group (ages 20−39) and the oldest age group (ages 60−79) differed significantly in their Aβ ratio ($p < 0.01$). This indicates that Aβ concentrations in the population of different age groups are related to a certain significant degree.

CONCLUSIONS

In this research, we chose an electrochemical impedance spectroscopy biosensor, even though this technique has been employed in many fields in the past few decades. However, the existing AD detection techniques (for example, high-performance liquid chromatography (HPLC), mass spectrometry (MS), enzyme-linked immunosorbent assay (ELISA), etc.) require a great quantity of samples. These techniques have some detection restrictions and are too expensive or time-

https://doi.org/10.1021/acs.analchem.0c04980
Anal. Chem. 2021, 93, 8099−8106

consuming to employ on early detection and wide-range screening. Consequently, our novel biosensors solve these problems. We can use samples sparingly and shorten the detection time to complete an examination. The excellent results show that the structure of the simple device for extracting tear fluid samples from Schirmer test strips is innovative, effective, and remarkable.

This study conducted a feasibility test for early detection of AD-associated biomarkers via detection of Aβ in blood and tears. The most important breakthrough in this study is that the concentration levels of Aβ among various age groups differed significantly. Aβ concentration in young healthy individuals is more than that in elderly people in both the testing samples of tear and blood. This proves that Aβ movement from peripheral tissues to the central nervous system with age occurs in all human beings regardless of whether they are suffering from AD or not. Another considerable discovery is that the concentration of Aβ in tears is 10 times more than that in blood. Therefore, tears might be a more practical specimen to be used for early detection due to their higher Aβ content and less invasiveness for patients.

The Aβ detection method demonstrated in this study can greatly reduce the cost of testing and discomfort of the subjects. Furthermore, it demonstrates the practicality of future screening for AD-associated biomarkers via the usage of blood and tears.

AUTHOR INFORMATION

Corresponding Author

Jung-Chih Chen − *Institute of Biomedical Engineering, National Chiao Tung University, Hsinchu 30010, Taiwan; Department of Electrical and Computer Engineering and Department of Biological Science and Technology, National Chiao Tung University, Hsinchu 30010, Taiwan;* orcid.org/0000-0003-3958-6806; Email: george@nctu.edu.tw

Authors

Yu-Rong Wang − *Institute of Biomedical Engineering, National Chiao Tung University, Hsinchu 30010, Taiwan*

Han-Chien Chuang − *Institute of Biomedical Engineering, National Chiao Tung University, Hsinchu 30010, Taiwan*

Adarsh Tripathi − *Institute of Molecular Medicine, National Tsing Hua University, Hsinchu 30010, Taiwan; Institute of Nanoengineering and Microsystems, National Tsing Hua University, Hsinchu 30010, Taiwan*

Yu-Lin Wang − *Institute of Nanoengineering and Microsystems and Department of Power Mechanical Engineering, National Tsing Hua University, Hsinchu 30010, Taiwan;* orcid.org/0000-0002-4791-936X

Mei-Lan Ko − *Department of Ophthalmology, National Taiwan University Hospital Hsin-Chu Branch, Hsinchu 30010, Taiwan; Department of Biomedical Engineering and Environmental Sciences, National Tsing Hua University, Hsinchu 30010, Taiwan*

Ching-Cheng Chuang − *Institute of Biomedical Engineering, National Chiao Tung University, Hsinchu 30010, Taiwan; Department of Electrical and Computer Engineering, National Chiao Tung University, Hsinchu 30010, Taiwan*

Complete contact information is available at: https://pubs.acs.org/10.1021/acs.analchem.0c04980

Notes

The authors declare no competing financial interest.

ACKNOWLEDGMENTS

This work was supported partially by the Taiwan Ministry of Science and Technology under Grant MOST 105-2221-E-009-093 and MOST 109-2221-E-009 -008 -MY3. In addition, this paper was particularly supported by the National Taiwan University Hospital Hsin-Chu Branch (NTUHHCB) (NTUHHCB 107-HCH061).

REFERENCES

(1) Prince, M.; Wimo, A.; Guerchet, M.; Ali, G.; Wu, Y.; Prina, M. *World Alzheimer Report 2015. The Global Impact of Dementia*; Alzheimer's Disease International (ADI): London, 2015.

(2) Jindal, H.; Bhatt, B.; Sk, S.; Singh Malik, J. *Hum. Vaccines Immunother.* **2014**, *10*, 2741−2743.

(3) Sadigh-Eteghad, S.; Sabermarouf, B.; Majdi, A.; Talebi, M.; Farhoudi, M.; Mahmoudi, J. *Med. Princ. Pract.* **2015**, *24*, 1−10.

(4) Blennow, K.; Zetterberg, H.; Fagan, A. M. *Cold Spring Harbor Perspect. Med.* **2012**, *2*, No. a006221.

(5) Katzman, R. *Neurobiol. Aging* **1989**, *10*, 581−582.

(6) Lee, H.-g.; Perry, G.; Moreira, P. I.; Garrett, M. R.; Liu, Q.; Zhu, X.; Takeda, A.; Nunomura, A.; Smith, M. A. *Trends Mol. Med.* **2005**, *11*, 164−169.

(7) Raina, P.; Santaguida, P.; Ismaila, A.; Patterson, C.; Cowan, D.; Levine, M.; Booker, L.; Oremus, M. *Ann. Intern. Med.* **2008**, *148*, 379−397.

(8) Olivares, D.; K Deshpande, V.; Shi, Y.; K Lahiri, D.; H Greig, N.; T Rogers, J.; Huang, X. *Curr. Alzheimer Res.* **2012**, *9*, 746−758.

(9) Jack, C. R., Jr.; Bennett, D. A.; Blennow, K.; Carrillo, M. C.; Dunn, B.; Haeberlein, S. B.; Holtzman, D. M.; Jagust, W.; Jessen, F.; Karlawish, J.; et al. *Alzheimer's Dementia* **2018**, *14*, 535−562.

(10) Fagan, A. M.; Mintun, M. A.; Mach, R. H.; Lee, S. Y.; Dence, C. S.; Shah, A. R.; LaRossa, G. N.; Spinner, M. L.; Klunk, W. E.; Mathis, C. A.; et al. *Ann. Neurol.* **2006**, *59*, 512−519.

(11) Grimmer, T.; Riemenschneider, M.; Förstl, H.; Henriksen, G.; Klunk, W. E.; Mathis, C. A.; Shiga, T.; Wester, H.-J.; Kurz, A.; Drzezga, A. *Biol. Psychiatry* **2009**, *65*, 927−934.

(12) Strozyk, D.; Blennow, K.; White, L.; Launer, L. *Neurology* **2003**, *60*, 652−656.

(13) Tapiola, T.; Alafuzoff, I.; Herukka, S.-K.; Parkkinen, L.; Hartikainen, P.; Soininen, H.; Pirttilä, T. *Arch. Neurol.* **2009**, *66*, 382−389.

(14) van Oijen, M.; Hofman, A.; Soares, H. D.; Koudstaal, P. J.; Breteler, M. M. *Lancet Neurol.* **2006**, *5*, 655−660.

(15) Lee, J. C.; Kim, S. J.; Hong, S.; Kim, Y. *Exp. Mol. Med.* **2019**, *51*, 1−10.

(16) Mehta, P. D.; Pirttilä, T.; Mehta, S. P.; Sersen, E. A.; Aisen, P. S.; Wisniewski, H. M. *Arch. Neurol.* **2000**, *57*, 100−105.

(17) Selkoe, D. J. *Nature* **1999**, *399*, A23−A31.

(18) Shioi, J.; Georgakopoulos, A.; Mehta, P.; Kouchi, Z.; Litterst, C. M.; Baki, L.; Robakis, N. K. *J. Neurochem.* **2007**, *101*, 674−681.

(19) Opazo, C.; Huang, X.; Cherny, R. A.; Moir, R. D.; Roher, A. E.; White, A. R.; Cappai, R.; Masters, C. L.; Tanzi, R. E.; Inestrosa, N. C.; et al. *J. Biol. Chem.* **2002**, *277*, 40302−40308.

(20) Hagan, S.; Martin, E.; Enríquez-de-Salamanca, A. *EPMA J.* **2016**, *7*, 15.

(21) Kalló, G.; Emri, M.; Varga, Z.; Ujhelyi, B.; Tőzsér, J.; Csutak, A.; Csősz, É. *PLoS One* **2016**, *11*, No. e0158000.

(22) Kenny, A.; Jiménez-Mateos, E. M.; Zea-Sevilla, M. A.; Rábano, A.; Gili-Manzanaro, P.; Prehn, J. H.; Henshall, D. C.; Ávila, J.; Engel, T.; Hernández, F. *Sci. Rep.* **2019**, *9*, No. 15437.

(23) Santos, C. Y.; Johnson, L. N.; Sinoff, S. E.; Festa, E. K.; Heindel, W. C.; Snyder, P. J. *Alzheimer's Dementia: Diagn., Assess. Dis. Monit.* **2018**, *10*, 196−209.

(24) Koronyo, Y.; Salumbides, B. C.; Black, K. L.; Koronyo-Hamaoui, M. *Neurodegener. Dis.* **2012**, *10*, 285−293.

(25) Moncaster, J. A.; Pineda, R.; Moir, R. D.; Lu, S.; Burton, M. A.; Ghosh, J. G.; Ericsson, M.; Soscia, S. J.; Mocofanescu, A.; Folkerth, R. D.; et al. *PLoS One* **2010**, *5*, No. e10659.
(26) Goldstein, L. E.; Muffat, J. A.; Cherny, R. A.; Moir, R. D.; Ericsson, M. H.; Huang, X.; Mavros, C.; Coccia, J. A.; Faget, K. Y.; Fitch, K. A.; et al. *Lancet* **2003**, *361*, 1258−1265.
(27) Frederikse, P. H.; Garland, D.; Zigler, J. S.; Piatigorsky, J. *J. Biol. Chem.* **1996**, *271*, 10169−10174.
(28) Wright, L. M.; Stein, T. D.; Jun, G.; Chung, J.; McConnell, K.; Fiorello, M.; Siegel, N.; Ness, S.; Xia, W.; Turner, K. L.; et al. *J. Alzheimer's Dis.* **2019**, *68*, 1429−1438.
(29) Chuah, K.; Lai, L. M.; Goon, I. Y.; Parker, S. G.; Amal, R.; Gooding, J. J. *Chem. Commun.* **2012**, *48*, 3503−3505.
(30) Yoo, M.-S.; Shin, M.; Kim, Y.; Jang, M.; Choi, Y.-E.; Park, S. J.; Choi, J.; Lee, J.; Park, C. *Chemosphere* **2017**, *175*, 269−274.
(31) Pasta, M.; La Mantia, F.; Cui, Y. *Electrochim. Acta* **2010**, *55*, 5561−5568.
(32) Chidsey, C. E.; Loiacono, D. N. *Langmuir* **1990**, *6*, 682−691.
(33) Florea, A.; Guo, Z.; Cristea, C.; Bessueille, F.; Vocanson, F.; Goutaland, F.; Dzyadevych, S.; Săndulescu, R.; Jaffrezic-Renault, N. *Talanta* **2015**, *138*, 71−76.
(34) Rushworth, J. V.; Ahmed, A.; Griffiths, H. H.; Pollock, N. M.; Hooper, N. M.; Millner, P. A. *Biosens. Bioelectron.* **2014**, *56*, 83−90.
(35) Zhou, Y.; Zhang, H.; Liu, L.; Li, C.; Chang, Z.; Zhu, X.; Ye, B.; Xu, M. *Sci. Rep.* **2016**, *6*, No. 35186.
(36) Carneiro, P.; Loureiro, J.; Delerue-Matos, C.; Morais, S.; do Carmo Pereira, M. *Sens. Actuators, B* **2017**, *239*, 157−165.
(37) Wu, C.-C.; Ku, B.-C.; Ko, C.-H.; Chiu, C.-C.; Wang, G.-J.; Yang, Y.-H.; Wu, S.-J. *Electrochim. Acta* **2014**, *134*, 249−257.
(38) Gijs, M.; Ramakers, I. H.; Visser, P. J.; Verhey, F. R.; van de Waarenburg, M. P.; Schalkwijk, C. G.; Nuijts, R. M.; Webers, C. A. Detection of amyloid-beta and tau in tear fluid of patients with Alzheimer's disease, **2020**, DOI: 10.21203/rs.3.rs-36499/v1.

https://doi.org/10.1021/acs.analchem.0c04980
Anal. Chem. 2021, 93, 8099−8106